Proceedings of ALGORITMY 2000
Conference on Scientific Computing, pp. 37–46

MATHEMATICAL DESCRIPTION OF SOFT TISSUE MECHANICS

JAROSLAV HRON*

Abstract. In this work we investigate a mathematical model for the description of the mechanical behavior of soft, hydrated tissues with significant perfusion. We set up and derive the mathematical description and balance laws using the continuum mixture theory as the theoretical framework. The constitutive relations suitable to describe perfused soft tissue and appropriate boundary conditions are discussed. We solve illustrative steady, one and two dimensional problems of diffusion through finitely deformed slab, and develop an algorithm based on finite element method for finding approximate solution to the continuous, nonlinear, steady, two dimensional problem.

Key words. finite elements, soft tissue, mixture

AMS subject classifications. 74A20, 74A50, 76Z, 74F

1. Introduction. The ability to model and predict the mechanical behavior of biological tissues is very important in several areas of bio-engineering and medicine. For example, a good mathematical model for biological tissue could be used in such areas as early recognition or prediction of heart muscle failure, advanced design of new treatments and operative procedures, and the understanding of atherosclerosis and associated problems. Other possible applications include development of virtual reality programs for training new surgeons or designing new operative procedures [9], and last but not least the design of medical instruments or artificial replacements with mechanical and other properties as close as possible to the original parts. These are some of the areas where a good mathematical model of soft tissue is essential for success.

Muscle tissue consists of muscle fibers and capillary blood vessels aligned in one direction and amorphous extracellular matrix and interstitial fluid which fills the voids and is limited in its movement. The size of the capillaries is of the order of the diameter of the red blood cell and their distribution in the muscle tissue is regular. This fact allows us to use some kind of homogenization to describe the material. The uni-directional orientation of the muscle fibers also suggests that transversely isotropic symmetry is appropriate. An overview of models for soft tissues including models of active muscle contraction is presented in [4] and [7]. Since a mathematical description of such materials on a microscopical level would be too complicated, other means of description are used to describe mathematically the mechanics of such materials.

A typical experiment we would like to model is the biaxial stretching of a muscle specimen, see figure 1.1, with simultaneous perfusion through the capillaries. Some of the characteristic properties in such problem are:

- The tissue specimen in the experiment, and even in its natural environment, is subjected to large deformation.
- Muscle fibers in the specimen are oriented in one direction.
- The perfusion takes place through parallel capillaries.
- The perfusion flow can have significant velocity possibly varying in time.
- The diameter of the capillary is comparable with the diameter of the red blood cell. ($\approx 5\mu$m)

*Mathematical Institute of Charles University, Sokolovská 83, 186 00 Praha 8, Czech Republic

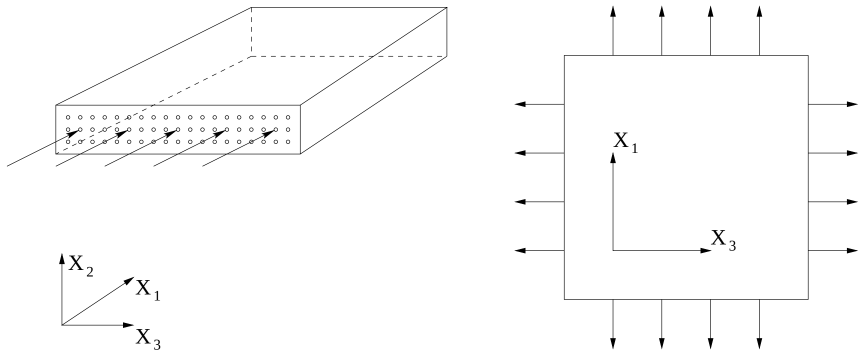

FIG. 1.1. *Schematic view of biaxial stretching experiment and muscle perfusion.*

- The distribution of the capillaries is regular.

The continuum assumption has proven to be a very useful tool in fluid and solid mechanics. It idealizes the body of interest, consisting of individual particles (atoms or molecules), as a continuous region in space. There has to be certain conditions in order to use this approach, namely the characteristic size of the body and the disturbances imposed on the body have to be "much" greater than the size of the individual particles.

Similar ideas support the mixture theory. In the mixture, each of the constituents is treated as a continuum occupying the whole volume of the mixture. The connection with the real mixture can be established through a homogenization procedure. Clearly, the validity of such treatment can be expected only when the characteristic size of the structural constitution of the mixture (i.e. atomic or molecular level mixture, size of the particles of granular mixture, or size of the pores in porous media) is "much" smaller than the characteristic size of the mixture body and the size of the disturbances imposed on the body.

2. Binary mixture of a solid and a fluid. Let us now focus on the diffusion of one fluid through an incompressible homogeneous elastic solid subjected to a finite deformation, without external body forces. The motion of each constituent of the mixture is described by mappings

$$\boldsymbol{\chi}^s(\boldsymbol{X}^s, t) : \Omega^s \times [0, T] \mapsto \Omega \tag{2.1}$$

$$\boldsymbol{\chi}^f(\boldsymbol{X}^f, t) : \Omega^f \times [0, T] \mapsto \Omega \tag{2.2}$$

where the superscripts s and f refer to quantities associated with the solid and fluid, respectively, Ω is the domain occupied by the mixture and Ω^s and Ω^f represents the reference configuration of both components. At each time $t \in [0, T]$, the mappings are one-to-one and sufficiently smooth to render the various mathematical operations meaningful.

2.1. Balance equations. We denote by ϱ^s and ϱ^f the partial densities of the solid and fluid, respectively. The total density of the mixture is given by $\varrho = \varrho^s + \varrho^f$. The deformation gradient for the solid is given by $\mathsf{F} = \frac{\partial \boldsymbol{x}^s}{\partial \boldsymbol{X}^s}$ where $\boldsymbol{x}^s = \boldsymbol{\chi}^s(\boldsymbol{X}^s, t)$ is the current position of particle occupying position $\boldsymbol{X}^s$ in the reference configuration, and the velocity vector of the solid $\boldsymbol{v}^s = \frac{\partial \boldsymbol{x}^s}{\partial t}$. In the absence of inter conversion between the constituents, the equation for the conservation of mass for the solid is

$$\frac{\partial \varrho^s}{\partial t} + \operatorname{div}(\varrho^s \boldsymbol{v}^s) = 0. \tag{2.3}$$

The conservation of mass (2.3) can also be expressed in the Lagrangian form

$$\varrho^s \det \mathbf{F} = \varrho_0^s, \tag{2.4}$$

where ϱ_0^s is the density of the solid in the undeformed state. Let $\boldsymbol{\sigma}^s$ and $\boldsymbol{\sigma}^f$ denote the partial stresses associated with the solid and fluid constituents, respectively, and $\boldsymbol{b}^s$ and $\boldsymbol{b}^f$ denote the interactive forces acting on the solid and fluid. The balance of linear momentum for the solid is given by

$$\frac{\partial(\varrho^s \boldsymbol{v}^s)}{\partial t} + \operatorname{div}(\varrho^s \boldsymbol{v}^s \otimes \boldsymbol{v}^s) = \operatorname{div} \boldsymbol{\sigma}^s + \boldsymbol{b}^s. \tag{2.5}$$

For the fluid constituent we define the velocity $\boldsymbol{v}^f = \frac{\partial \boldsymbol{x}^f}{\partial t}$ and the conservation of mass and the balance of linear momentum for this constituent are

$$\frac{\partial \varrho^f}{\partial t} + \operatorname{div}(\varrho^f \boldsymbol{v}^f) = 0, \tag{2.6}$$

$$\frac{\partial(\varrho^f \boldsymbol{v}^f)}{\partial t} + \operatorname{div}(\varrho^f \boldsymbol{v}^f \otimes \boldsymbol{v}^f) = \operatorname{div} \boldsymbol{\sigma}^f + \boldsymbol{b}^f. \tag{2.7}$$

By the action-reaction principle we have $\boldsymbol{b} = \boldsymbol{b}^f = -\boldsymbol{b}^s$. For the mixture, we define the total stress $\boldsymbol{\sigma} = \boldsymbol{\sigma}^s + \boldsymbol{\sigma}^f$ which is symmetric as required by the balance of the angular momentum.

The entropy inequality for the mixture is used to restrict the class of constitutive forms for $\boldsymbol{\sigma}^s$, $\boldsymbol{\sigma}^f$ and $\boldsymbol{b}$. The reduced entropy inequality for the isothermal binary mixture can be written as

$$\frac{\partial(\varrho\Psi)}{\partial t} + \operatorname{div}(\varrho^s \Psi^s \boldsymbol{v}^s + \varrho^f \Psi^f \boldsymbol{v}^f) - \operatorname{tr}\left(\boldsymbol{\sigma}^s \operatorname{grad} \boldsymbol{v}^s + \boldsymbol{\sigma}^f \operatorname{grad} \boldsymbol{v}^f\right) + \boldsymbol{b} \cdot (\boldsymbol{v}^s - \boldsymbol{v}^f) \le 0, \tag{2.8}$$

where $\varrho\Psi = \varrho^s \Psi^s + \varrho^f \Psi^f$. For a detailed discussion of the above derivations and related issues we refer to [5], [8] and [10].

2.2. Kinematical constraints. The distribution of each constituent is described by the quantities ϕ^s and ϕ^f and can be interpreted as the volumetric amount of the constituent per unit volume of the mixture, i.e. volumetric concentrations. The volume additivity constraint for binary mixture

$$\phi^s + \phi^f = 1, \tag{2.9}$$

can be interpreted as requirement that the mixture consists only of these two components, not allowing voids. The true density of each constituent, denoted by ϱ_t^s and ϱ_t^f satisfy

$$\varrho^s = \phi^s \varrho_t^s, \qquad \varrho^f = \phi^f \varrho_t^f. \tag{2.10}$$

So far the quantities $\varrho^s, \varrho^f, \phi^s, \phi^f$ are independent unknown fields and we have to add some more additional assumptions to be able to determine them. We assume that the true densities of both constituents are constant, and effectively eliminates for example the densities ϱ^s, ϱ^f by (2.10), leaving us with the volume fractions ϕ^s, ϕ^f as the unknowns. Then the volume additivity requirement (2.9) has to be considered as an additional kinematical constraint. It implies together with equations (2.3), (2.6) and (2.9) that

$$\operatorname{div}(\phi^s \boldsymbol{v}^s + \phi^f \boldsymbol{v}^f) = 0. \tag{2.11}$$

2.3. Constitutive equations. We will restrict our considerations to isothermal, non-reacting mixtures where the solid constituent is homogeneous and hyperelastic. For such mixtures it can be shown, using the second law of thermodynamics and the postulate of material frame indifference, that the Helmholtz potential can be expressed as a function of the deformation tensor $\mathbf{C} = \mathbf{F}^T\mathbf{F}$ and the fluid volume fraction ϕ^f, i.e.,

$$\Psi = \hat{\Psi}(\mathbf{C}, \phi^f). \tag{2.12}$$

Using techniques that are standard in continuum mechanics (see [10]) we obtain an expression for the partial stresses $\boldsymbol{\sigma}^s$ and $\boldsymbol{\sigma}^f$ and the interaction force $\boldsymbol{b}$ such that the entropy inequality is satisfied for all admissible processes. If we choose the partial stresses to be given by

$$\boldsymbol{\sigma}^s = \frac{\varrho^s\varrho^f}{\varrho}(\hat{\Psi}^s - \hat{\Psi}^f)\mathbf{I} - \phi^s p\mathbf{I} + 2\varrho\mathbf{F}\frac{\partial\hat{\Psi}}{\partial\mathbf{C}}\mathbf{F}^T + \hat{\boldsymbol{\sigma}}^s \tag{2.13}$$

$$\boldsymbol{\sigma}^f = -\frac{\varrho^s\varrho^f}{\varrho}(\hat{\Psi}^s - \hat{\Psi}^f)\mathbf{I} - \phi^f p\mathbf{I} - \varrho\phi^f\frac{\partial\hat{\Psi}}{\partial\phi^f}\mathbf{I} + \hat{\boldsymbol{\sigma}}^f \tag{2.14}$$

and the interaction force to have the form

$$\boldsymbol{b} = -\nabla\left(\frac{\varrho^s\varrho^f}{\varrho}(\hat{\Psi}^s - \hat{\Psi}^f)\right) - p\nabla\phi^s + \varrho\frac{\partial\hat{\Psi}}{\partial\phi^f}\nabla\phi^f - \varrho^f\nabla\hat{\Psi} + \hat{\boldsymbol{b}}, \tag{2.15}$$

where $\hat{\boldsymbol{\sigma}}^f$, $\hat{\boldsymbol{\sigma}}^s$, $\hat{\boldsymbol{b}}$ are the parts of the partial stresses that depend only on the dynamical variables, i.e. $\boldsymbol{v}^s - \boldsymbol{v}^f$, $\nabla\boldsymbol{v}^s$, $\nabla\boldsymbol{v}^f$, then the entropy inequality reduces to

$$\operatorname{tr}\left(\hat{\boldsymbol{\sigma}}^s\mathbf{D}^s + \hat{\boldsymbol{\sigma}}^f\mathbf{D}^f + \hat{\boldsymbol{\sigma}}^s(\mathbf{W}^s - \mathbf{W}^f)\right) - \hat{\boldsymbol{b}}\cdot(\boldsymbol{v}^s - \boldsymbol{v}^f) \geq 0, \tag{2.16}$$

where $\mathbf{D}^s$, $\mathbf{W}^s$, $\mathbf{D}^f$, $\mathbf{W}^f$ denote the symmetric and skew-symmetric part of the velocity gradients.

For simplicity, let us set

$$\hat{\boldsymbol{\sigma}}^s = 0, \qquad \hat{\boldsymbol{\sigma}}^f = 0, \qquad \hat{\boldsymbol{b}} = \phi^s\phi^f\boldsymbol{\alpha}(\boldsymbol{v}^s - \boldsymbol{v}^f)$$

where $\boldsymbol{\alpha}$ is positive definite tensor and represents the drag coefficient between the fluid and solid, which is the dominant interaction. We shall assume that $\Psi = \tilde{\Psi}(I_C, II_C, \phi^s)$, where I_C, II_C are the first and second invariant of $\mathbf{C}$. Substituting these constitutive equations into the balance of linear momentum for the constituents, we obtain

$$\frac{\partial(\varrho^s\boldsymbol{v}^s)}{\partial t} + \operatorname{div}(\varrho^s\boldsymbol{v}^s\otimes\boldsymbol{v}^s) = -\phi^s\nabla p + \operatorname{div}\boldsymbol{\sigma}^E + \varrho^f\nabla\tilde{\Psi} - \phi^s\phi^f\boldsymbol{\alpha}(\boldsymbol{v}^s - \boldsymbol{v}^f), \tag{2.17}$$

$$\frac{\partial(\varrho^f\boldsymbol{v}^f)}{\partial t} + \operatorname{div}(\varrho^f\boldsymbol{v}^f\otimes\boldsymbol{v}^f) = -\phi^f\nabla p - \varrho^f\nabla\tilde{\Psi} + \phi^s\phi^f\boldsymbol{\alpha}(\boldsymbol{v}^s - \boldsymbol{v}^f), \tag{2.18}$$

with $\boldsymbol{\sigma}^E = 2\varrho\big[\frac{\partial\tilde{\Psi}}{\partial I_C}\mathbf{B} + \frac{\partial\tilde{\Psi}}{\partial II_C}(I_C\mathbf{B} - \mathbf{B}^2)\big] - \varrho\phi^s\frac{\partial\tilde{\Psi}}{\partial\phi^s}\mathbf{I}$. These equations together with the constraint (2.9), mass balance equations (2.4) and (2.6), suitable boundary conditions and specific form for the function $\tilde{\Psi}$ make complete problem to solve.

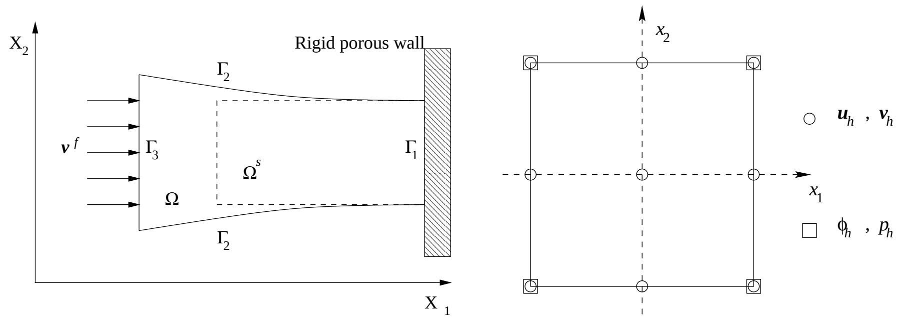

FIG. 3.1. *Undeformed and deformed configuration in two dimensional problem and the degrees of freedom on the reference element.*

3. Two dimensional problem. We formulate a solution algorithm for a steady state, two-dimensional problem of stretched rectangular slab of solid-fluid mixture. Some other formulations can be found in [1, 2, 3, 6, 11]. Let $\boldsymbol{u}$ denotes the solid displacement, $\boldsymbol{v}$ denotes the fluid velocity, ϕ is the fluid volume fraction and p is the Lagrange multiplier associated with the kinematical constraint (2.11). Let $\Omega^s = [-L, L] \times [-H, H] \times [-L, L]$ be the reference domain occupied by the solid. The deformed domain, shown in figure 3.1(a), is

$$\Omega = \{x = X + \boldsymbol{u}(X), \forall X \in \Omega^s\}. \tag{3.1}$$

The deformation is assumed to be of a form

$$x_1 = X_1 + u_1(X_1, X_2), \qquad x_2 = X_2 + u_2(X_1, X_2), \qquad x_3 = \lambda_3 X_3, \tag{3.2}$$

where λ_3 is prescribed positive constant. The fluid velocity is assumed to be

$$\boldsymbol{v}(x_1) = (v_1(x_1, x_2), v_2(x_1, x_2), 0). \tag{3.3}$$

Let the symbol ∇ stands for $\frac{\partial}{\partial X^s}$, then $\mathsf{F} = \mathsf{I} + \nabla \boldsymbol{u}$ and our task is to find $(\boldsymbol{u}, \boldsymbol{v}, \phi, p)$ such that

$$\phi(\operatorname{grad} \boldsymbol{v})\boldsymbol{v} + \operatorname{grad} p - \operatorname{div} \boldsymbol{\sigma}^E = 0 \tag{3.4}$$
$$(\operatorname{grad} \boldsymbol{v})\boldsymbol{v} + \operatorname{grad}(p + \Psi) + (1 - \phi)\boldsymbol{\alpha}\boldsymbol{v} = 0 \tag{3.5}$$
$$(1 - \phi) \det \mathsf{F} = \phi_0^s \tag{3.6}$$
$$\operatorname{div}(\phi \boldsymbol{v}) = 0 \tag{3.7}$$

holds in domain Ω, where ϕ_0^s is the volume fraction of the solid in the reference state and the Helmholtz potential Ψ is given by constitutive equation as a function of ϕ and F. The part of the Cauchy stress tensor $\boldsymbol{\sigma}$ is then given by

$$\boldsymbol{\sigma}^E = (\phi + \beta(1 - \phi)) \frac{\partial \Psi}{\partial \mathsf{F}} \mathsf{F}^T, \tag{3.8}$$

where $\beta = \frac{\varrho_t^s}{\varrho_t^f}$ is the true mass ratio.

Let the boundary $\partial\Omega$ be divided into three disjoint parts $\partial\Omega = \bigcup_{i=1}^{3} \Gamma_i$. Let $\boldsymbol{n}$ be the unit normal vector to the boundary $\partial\Omega$. Then if $\boldsymbol{t}$ is given traction on the boundary, $\boldsymbol{u}_B$ is given solid boundary displacement and $\boldsymbol{v}_B$ is given fluid velocity at the boundary the possible boundary conditions are

$$\frac{1}{3}\operatorname{tr}\boldsymbol{\sigma} = p_B, \quad \boldsymbol{u} = \boldsymbol{u}_B \quad \text{on } \Gamma_1, \tag{3.9}$$

$$-p\boldsymbol{n} + \boldsymbol{\sigma}^E\boldsymbol{n} = \boldsymbol{t}, \quad \boldsymbol{v} = \boldsymbol{v}_B \quad \text{on } \Gamma_2, \tag{3.10}$$

$$\boldsymbol{u} = \boldsymbol{u}_B, \quad \boldsymbol{v} = \boldsymbol{v}_B \quad \text{on } \Gamma_3. \tag{3.11}$$

We avoid prescribing partial stresses on the boundary since it is not clear weather such values can be obtained by measurements or how the total stress should be partitioned into the partial stresses. Instead, we focus on the prescription of such quantities that can be measured in experiments.

3.1. Weak formulation. In order to apply the finite element method we formulate our problem in a weak sense. Let us define spaces U, V, M and P as follows

$$U = \{\boldsymbol{u} \in [W^{1,2}(\Omega^s)]^2, \boldsymbol{u} = \boldsymbol{0} \text{ on } \Gamma_1 \cup \Gamma_3\}, \tag{3.12}$$

$$V = \{\boldsymbol{v} \in [W^{1,2}(\Omega^s)]^2, \boldsymbol{v} = 0 \text{ on } \Gamma_2 \cup \Gamma_3\}, \tag{3.13}$$

$$M = \{\phi \in W^{1,2}(\Omega^s), 0 \le \phi \le 1 \text{ in } \Omega\}, \tag{3.14}$$

$$P = \{p \in L^2(\Omega^s)\}. \tag{3.15}$$

Multiplying equations (3.4)–(3.7) by a test functions $(\boldsymbol{\zeta}, \boldsymbol{\xi}, \eta, \gamma)$, integrating over the domain Ω and using per-partes integration and transformation to the reference domain of the solid Ω^s we obtain

$$\begin{aligned}\int_{\Omega^s} \phi \nabla \boldsymbol{v} \operatorname{cof} \mathbf{F}^T \boldsymbol{v} \cdot \boldsymbol{\zeta} \, \mathrm{d}x - \int_{\Omega^s} p \operatorname{cof} \mathbf{F} \cdot \nabla \boldsymbol{\zeta} \, \mathrm{d}x + \int_{\Omega^s} \mathbf{S}^E \cdot \nabla \boldsymbol{\zeta} \, \mathrm{d}x& \\ - \int_{\Gamma_2} \boldsymbol{t} \operatorname{cof} \mathbf{F} \boldsymbol{N} \cdot \boldsymbol{\zeta} \, \mathrm{d}a = 0,&\end{aligned} \tag{3.16}$$

$$\begin{aligned}\int_{\Omega^s} \nabla \boldsymbol{v} \operatorname{cof} \mathbf{F} \boldsymbol{v} \cdot \boldsymbol{\xi} \, \mathrm{d}x - \int_{\Omega^s} (p + \Psi) \operatorname{cof} \mathbf{F} \cdot \nabla \boldsymbol{\xi} \, \mathrm{d}x + \int_{\Omega^s} (1 - \phi) \boldsymbol{\alpha} \boldsymbol{v} \cdot \boldsymbol{\xi} \det \mathbf{F} \, \mathrm{d}x& \\ + \int_{\Gamma_1} (p_B - \frac{1}{3} \operatorname{tr} \boldsymbol{\sigma} + \Psi) \operatorname{cof} \mathbf{F} \boldsymbol{N} \cdot \boldsymbol{\xi} \, \mathrm{d}a = 0,&\end{aligned} \tag{3.17}$$

$$\int_{\Omega^s} ((1 - \phi) \det \mathbf{F} - \phi_0^s) \, \eta \, \mathrm{d}x = 0, \tag{3.18}$$

$$\int_{\Omega^s} \nabla (\phi \boldsymbol{v}) \cdot \operatorname{cof} \mathbf{F} \gamma \, \mathrm{d}x = 0, \tag{3.19}$$

where $\operatorname{cof} \mathbf{F} = \det \mathbf{F} \ \mathbf{F}^{-T}$ and the inner product for two tensors is defined as $\mathbf{F} \cdot \mathbf{G} = \operatorname{tr}(\mathbf{F}^T \mathbf{G})$. Then our task is to find $(\boldsymbol{u}, \boldsymbol{v}, \phi, p)$ such that $(\boldsymbol{u} - \boldsymbol{u}_B, \boldsymbol{v} - \boldsymbol{v}_B, \phi, p) \in U \times V \times M \times P$ and equations (3.16)–(3.19) are satisfied for all $(\boldsymbol{\zeta}, \boldsymbol{\xi}, \eta, \gamma) \in U \times V \times M \times P$.

3.2. Finite element discretization. The reference domain Ω^s is approximated by a domain Ω_h with piecewise linear boundary. The interior is divided by regular quadrilateral mesh into convex quadrilateral elements. Any two elements have in common either whole side, vertex or are disjoint. Let the set of all quadrilaterals in

1. Let $\boldsymbol{X}^n$ be some starting guess.
2. Set the residuum vector $\boldsymbol{R} = \quad (\boldsymbol{X}^n)$ and the tangent matrix $\mathsf{A} = \frac{\partial \mathcal{R}}{\partial \boldsymbol{X}}(\boldsymbol{X}^n)$.
3. Solve for the correction $\delta \boldsymbol{X}$

$$\mathsf{A} \delta \boldsymbol{X} = \boldsymbol{R}.$$

4. Update the solution $\boldsymbol{X}^{n+1} = \boldsymbol{X}^n - \omega \delta \boldsymbol{X}$.

FIG. 3.2. *One step of the Newton method.*

Ω_h be denoted by $\mathcal{T}_h$ and let $\tilde{T} = (-1,1)^2$ be the reference quadrilateral. For each element $T \in \mathcal{T}_h$ there is a bilinear one to one mapping on to the reference element $\tilde{T}$. The spaces U, V, M resp. P are approximated by finite element spaces

$$U_h = \{\boldsymbol{u}_h \in [C(\Omega_h)]^2, \boldsymbol{u}_h|T \in [Q_2(T)]^2 \quad \forall T \in \mathcal{T}_h, \boldsymbol{u}_h = \boldsymbol{0} \text{ on } \Gamma_1 \cup \Gamma_3\}, \tag{3.20}$$

$$V_h = \{\boldsymbol{v}_h \in [C(\Omega_h)]^2, \boldsymbol{v}_h|T \in [Q_2(T)]^2 \quad \forall T \in \mathcal{T}_h, \boldsymbol{v}_h = 0 \text{ on } \Gamma_1 \cup \Gamma_3\}, \tag{3.21}$$

$$M_h = \{\phi_h \in C(\Omega_h), \phi_h|T \in Q_1(T) \quad \forall T \in \mathcal{T}_h, 0 \le \phi_h \le 1\}, \tag{3.22}$$

$$P_h = \{p_h \in C(\Omega_h), p_h|T \in Q_1(T) \quad \forall T \in \mathcal{T}_h\}. \tag{3.23}$$

Where $Q_n(T)$ denotes the space of polynomial functions, defined on the quadrilateral T, which transformed to the reference element $\tilde{T}$ are polynomials of order at most n in each reference coordinate. The location of local degrees of freedom on the reference element is shown in figure 3.1(b). The resulting discrete problem is obtained by taking usual nodal basis of the space $U_h \times V_h \times M_h \times P_h$ and using the elements of this basis as test functions $(\boldsymbol{\zeta}, \boldsymbol{\xi}, \eta, \gamma)$ in (3.16–3.19). This set of non-linear algebraic equations can be written as

$$(\boldsymbol{X}) = \boldsymbol{0}, \tag{3.24}$$

where $\boldsymbol{X} = (\boldsymbol{u}_h, \boldsymbol{v}_h, \phi_h, p_h)$ is the vector of unknown components. The corresponding linearized problem is to find $\delta \boldsymbol{X}$ such that

$$\left[\frac{\partial}{\partial \boldsymbol{X}}(\boldsymbol{X})\right] \delta \boldsymbol{X} = 0, \tag{3.25}$$

where the Jacobian matrix $\left[\frac{\partial \mathcal{R}}{\partial \boldsymbol{X}}(\boldsymbol{X})\right]$ has the typical structure of constraint system

$$\left[\frac{\partial}{\partial \boldsymbol{X}}(\boldsymbol{X})\right] = \begin{pmatrix} \mathsf{A}_{u,u} & \mathsf{A}_{u,v} & \mathsf{B}_{u,\phi} & \mathsf{C} \\ \mathsf{A}_{v,u} & \mathsf{A}_{v,v} & \mathsf{B}_{v,\phi} & \mathsf{C} \\ (1-\phi)\mathsf{C}^T & \mathbf{0} & \mathsf{B}_{\phi,\phi} & \mathbf{0} \\ \mathsf{A}_{p,u} & \phi\mathsf{C}^T & \mathsf{B}_{p,\phi} & \mathbf{0} \end{pmatrix}. \tag{3.26}$$

3.3. Solution algorithm. The system (3.24) of nonlinear algebraic equations is solved using damped Newton method as the basic iteration. One step of the Newton iteration is described in scheme 3.2. The parameter ω is adaptively found such, that certain error measure decreases. One of the possible choices for the quantity to decrease is

$$f(\omega) = \quad (\boldsymbol{X}^n + \omega \delta \boldsymbol{X}) \cdot \delta \boldsymbol{X}. \tag{3.27}$$

Minimizing quadratic approximation of $f(\omega)$

$$f(\omega)=\frac{f(\omega_0)-f(0)(\omega_0+1)}{\omega_0^2}\omega^2+f(0)(\omega+1), \tag{3.28}$$

yields optimal $\omega \in [-1,0]$ as

$$\omega=\begin{cases}-\dfrac{\tilde\omega}{2} & \text{if } \dfrac{f(0)}{f(\omega_0)}>0,\\ -\dfrac{\tilde\omega}{2}-\sqrt{\dfrac{\tilde\omega^2}{4}-\tilde\omega} & \text{if } \dfrac{f(0)}{f(\omega_0)}\le 0,\end{cases} \tag{3.29}$$

where

$$\tilde\omega=\frac{f(0)\omega_0^2}{f(\omega_0)-f(0)(\omega_0+1)}. \tag{3.30}$$

This line search can be repeated with ω_0 taken as the last ω until, for example, $f(\omega)\le(\omega+\frac{3}{2})f(0)$.

Additionally, the continuation method is employed in order to have the starting approximation in the Newton iteration in the range of convergence. In the continuation method the problem $\boldsymbol{F}(\boldsymbol{X})=0$ is replaced by

$$\boldsymbol{G}(\boldsymbol{X},\lambda)=0 \tag{3.31}$$

where λ is a parameter such that for $\boldsymbol{G}(\boldsymbol{X},0)=0$ we know the solution, while for $\lambda=1$ the original problem is recovered

$$\boldsymbol{G}(\boldsymbol{X},1)\equiv\boldsymbol{F}(\boldsymbol{X}). \tag{3.32}$$

For example making the boundary conditions to depend on the parameter λ in such a way that for $\lambda=0$ we have the undeformed, stress free state, and for $\lambda=1$ we have the original boundary conditions.

In the process of the continuation method, we follow the solution curve given by the initial value problem

$$\frac{\mathrm{d}}{\mathrm{d}s}\boldsymbol{G}(\boldsymbol{X}(s),\lambda(s))=0, \tag{3.33}$$

$$(\boldsymbol{X}(0),\lambda(0))=(\boldsymbol{X}_0,0), \tag{3.34}$$

until the point $\lambda(s)=1$. The basic method used to solve this problem is the Euler-Newton iteration, outlined in scheme 3.3, where the explicit Euler method is applied to (3.33) as predictor and then the solution is corrected by the Newton method. This step is repeated until $\lambda^n=1$. The parameter γ in the update step can be fixed or can be chosen adaptively, for example depending on the number of Newton iterations in the correction step needed to correct the solution.

The jacobian matrix is computed via finite differences. To invert the matrices in the most inner loops, BiCGStab or GMRES methods are used with suitable preconditioning. The incomplete LU decomposition is used for preconditioning with suitable ordering of unknowns and with allowed fill-in for certain pattern in the zero diagonal block of the jacobian matrix.

1. Let $\boldsymbol{X}^n$ be given starting approximation and λ^n the value of the continuation parameter.
2. Predictor step. Solve for $(\dot{\boldsymbol{X}}^n, \dot{\lambda^n})$

$$\left[\frac{\partial \boldsymbol{G}}{\partial \boldsymbol{X}}(\boldsymbol{X}^n, \lambda^n)\right] \dot{\boldsymbol{X}}^n + \left[\frac{\partial \boldsymbol{G}}{\partial \lambda}(\boldsymbol{X}^n, \lambda^n)\right] \dot{\lambda^n} = 0, \tag{3.35}$$

$$\|(\dot{\boldsymbol{X}}^n, \dot{\lambda^n})\| = 1. \tag{3.36}$$

3. Update the solution $(\boldsymbol{X}^{n+\frac{1}{2}}, \lambda^{n+1}) = (\boldsymbol{X}^n, \lambda^n) + \gamma(\dot{\boldsymbol{X}}^n, \dot{\lambda^n})$.
4. Correction step. Solve for $\boldsymbol{X}^{n+1}$ by Newton iteration with $\boldsymbol{X}^{n+\frac{1}{2}}$ as starting guess

$$\boldsymbol{G}(\boldsymbol{X}^{n+1}, \lambda^{n+1}) = 0. \tag{3.37}$$

FIG. 3.3. *One step of Euler-Newton algorithm.*

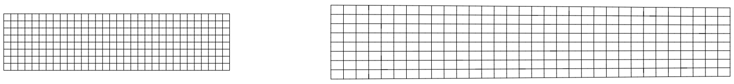

FIG. 3.4. *Finite element grid on the undeformed and deformed configuration of the solid.*

3.4. Illustrative example of perfusion. We take two dimensional crossection of the slab along the direction of the perfusion and assume the constitutive relation for the Helmholtz potential

$$\Psi = c_1(I_C - 3) + c_2 \ln(\phi). \tag{3.38}$$

The boundary conditions applied are $\boldsymbol{u} = \boldsymbol{u}_B, \quad \phi \boldsymbol{v} = \boldsymbol{v}_B$ at the left end of the specimen, $u_1 = 0, \sigma_{12} = 0, \frac{1}{3}\operatorname{tr}\boldsymbol{\sigma} = p_B$ at right end of the specimen and $\boldsymbol{\sigma n} = \boldsymbol{0}, \quad \phi \boldsymbol{v} = \boldsymbol{v}_B$ at the top and bottom parts.

In figure 3.4(a) we shown the finite element grid on the reference configuration of the solid. The initial solution is taken to be zero displacement and velocity, given constant volume fraction and lagrange multiplier p such that the solution is stress free. In figure 3.4(b) we show the finite element grid on the stretched configuration of the solid. We can see that the slab becomes thicker in the X_2 direction at the left end, and thinner at the fluid outflow end. This variation in the thickness is caused by the gradual decrease in the pressure along the fluid flow. Figure 3.5 shows the velocity field of the perfusion and the fluid volume fraction throughout the slab. The fluid velocity increases toward the end of the slab while the volume fraction decreases. In figure 3.6 the pressure field and the components of the stress tensor are depicted. We can notice the presence of stress concentration around the corners of the slab where the type of the boundary condition changes.

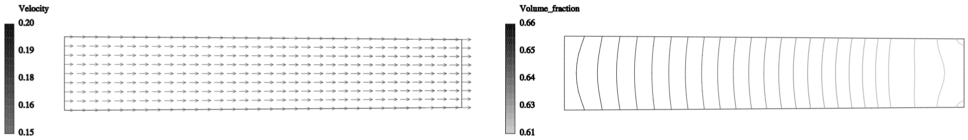

FIG. 3.5. *Fluid velocity field and the isolines of the fluid volume fraction.*

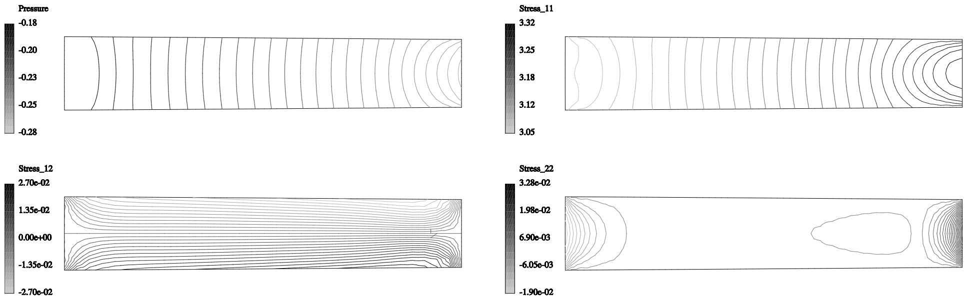

FIG. 3.6. *Isolines of the pressure and the stress components* $\sigma_{11}, \sigma_{12}, \sigma_{22}$.

REFERENCES

[1] E. S. ALMEIDA AND R. L. SPILKER, *Finite element formulations for hyperelastic transversely isotropic biphasic soft tissues*, Comp. Meth. Appl. Mech. Engng., 151 (1998), pp. 513–538.

[2] P. S. DONZELLI, R. L. SPILKER, P. L. BAEHMANN, Q. NIU, AND M. S. SHEPHARD, *Automated adaptive analysis of the biphasic equations for soft tissue mechanics using a posteriori error indicators*, Int. J. Numer. Meth. Engng., 34 (1992), pp. 1015–1033.

[3] W. EHLERS AND J. KUBIK, *On finite dynamic equations for fluid-saturated porous media*, Acta Mechanica, 105 (1994), pp. 101–117.

[4] Y. C. FUNG, *Biomechanics: Mechanical properties of living tissues*, Springer-Verlag, New York, NY, 2nd ed., 1993.

[5] A. E. GREEN AND P. M. NAGHDI, *A dynamical theory of interacting continua*, Int. J. Engng. Sci., 3 (1965), pp. 231–241.

[6] M. E. LEVENSTON, E. H. FRANK, AND A. J. GRODZINSKY, *Variationally derived 3-field finite element formulations for quasistatic poroelastic analysis of hydrated biological tissues*, Comp. Meth. Appl. Mech. Engng., 156 (1998), pp. 231–246.

[7] W. MAUREL, Y. WU, N. MAGNENAT THALMANN, AND D. THALMANN, *Biomechanical models for soft tissue simulation*, ESPRIT basic research series, Springer-Verlag, Berlin, 1998.

[8] I. MÜLLER, *A thermodynamic theory of mixtures of fluids*, Arch. Rational Mech. Anal., 28 (1967), pp. 1–39.

[9] K. D. PAULSEN, M. I. MIGA, F. E. KENNEDY, P. J. HOOPES, A. HARTOV, AND D. W. ROBERTS, *A computational model for tracking subsurface tissue deformation during stereotactic neurosurgery*, IEEE Transactions on Biomedical Engineering, 46 (1999), pp. 213–225.

[10] K. R. RAJAGOPAL AND L. TAO, *Mechanics of mixtures*, World Scientific Publishing Co. Inc., River Edge, NJ, 1995.

[11] J. K. SUH, R. L. SPILKER, AND M. H. HOLMES, *Penalty finite element analysis for non-linear mechanics of biphasic hydrated soft tissue under large deformation*, Int. J. Numer. Meth. Engng., 32 (1991), pp. 1411–1439.